Active noise control systems with optimized secondary path

Conference Paper · October 2004

DOI: 10.1109/CCA.2004.1387306 · Source: IEEE Xplore

2 authors:

Sen M. Kuo
Northern Illinois University
217 PUBLICATIONS **8,564** CITATIONS
SEE PROFILE

Woon-Seng Gan
Nanyang Technological University Singapore
555 PUBLICATIONS **8,362** CITATIONS
SEE PROFILE

Active Noise Control Systems with Optimized Secondary Path

Sen M. Kuo
Dept. of Electrical Engineering
Northern Illinois University
DeKalb, IL 60115
kuo@ceet.niu.edu

Woon S. Gan
School of Electrical & Electronic Engineering
NanyangTechnological University
Singapore 639798
EWSGAN@ntu.edu.sg

Abstract - In many real-world active noise control (ANC) applications such as electronic mufflers, the sensors may not be placed at the optimum locations in order to protect them from the high temperature, fast airflow, and corrosive environment. This paper presents an optimized algorithm for compensating sensor placement effects when the error sensor is placed at a secured physical location. This algorithm uses a compensation filter for pre-filtering the anti-noise such that the ANC system with the error sensor located at the physical location has the optimized secondary path as the sensor placed at the virtual location. An electronic muffler has been built and used for testing this optimized ANC system using engine noise. Computer simulations show significant improvement of the performance for the new ANC system with the optimized virtual secondary path.

I. INTRODUCTION

Noise problems become more and more evident by the increased number of industrial equipment in use. Noise can be reduced using passive techniques such as enclosures, barriers, and silencers. These passive techniques can attenuate noises over a broad frequency range, but they become expensive and ineffective for low frequency noises. The drawbacks of passive techniques have motivated the development of active noise control [1-4] based on the principle of superposition. In ANC systems, secondary sources are used to produce anti-noise with the same amplitude but the opposite phase of the primary noise in order to cancel the undesired noise. The amount of noise reduction achieved by an ANC system depends on the accuracy of the amplitude and phase of the generated anti-noise. Real-world applications require digital implementations of ANC systems using the advanced digital signal processors [5] for achieving satisfactory performance.

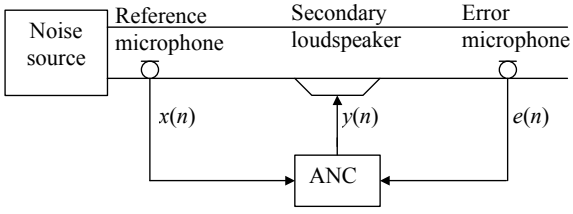

Figure 1 Single-channel ANC system in a duct

As illustrated in Figure 1, a single-channel broadband ANC system uses the reference microphone to pick up the undesired noise from the noise source. The reference signal, $x(n)$, is processed by the ANC system to generate the anti-noise, $y(n)$, which is output to the secondary loudspeaker for canceling the undesired noise in the duct. The residual noise $e(n)$ is picked by the error microphone, which is used to update the coefficients of the adaptive filter in the ANC system.

The ANC system shown in Figure 1 can be modeled using the block diagram in Figure 2, where $P(z)$ is the primary path transfer function from the reference microphone to the error microphone. The secondary path transfer function $S(z)$ includes the D/A converter, reconstruction filter, power amplifier, loudspeaker, acoustic path from the loudspeaker to the error microphone, error microphone, preamplifier, antialiasing filter, and A/D converter. The adaptive filter $W(z)$ minimizes the error signal $e(n)$, which is the residual noise measured by the error microphone. The acoustic domain in Figure 2 represents physical systems that include the primary and secondary paths and the acoustic summing junction for noise cancellation, while the electronic domain illustrates the ANC algorithm implemented on a digital signal processing system for real-time applications.

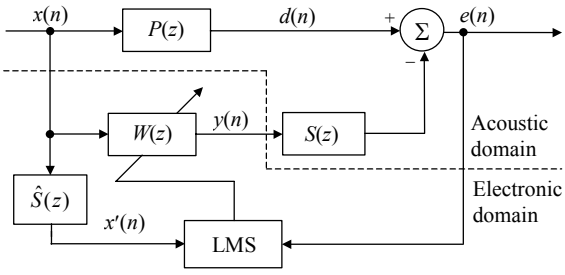

Figure 2 ANC system with the FXLMS algorithm

The least-mean-square (LMS) algorithm [6] used for many adaptive filtering applications should be modified for ANC systems that have the secondary path $S(z)$ after the adaptive filter $W(z)$. Two methods are proposed by Morgan [7] for solving this problem, and the most effective one uses the secondary-path estimate $\hat{S}(z)$ to filter $x(n)$ before reaching the LMS block as shown in

Figure 2. This modified algorithm is called the filtered-X LMS (FXLMS) algorithm [8], and was first used by Burgess [9] for ANC applications.

As shown in Figure 2, the adaptive filter generates the anti-noise $y(n)$ by filtering the reference signal $x(n)$ expressed as

$$y(n) = \mathbf{w}^T(n)\mathbf{x}(n), \quad (1)$$

where T denotes the transpose of the vector, $\mathbf{w}(n) = [w_0(n)\ w_1(n)\ \cdots\ w_{L-1}(n)]^T$ is the coefficient vector at time n, L is the order of the filter, and $\mathbf{x}(n) = [x(n)\ x(n-1)\ \cdots\ x(n-L+1)]^T$ is the signal vector. The adaptive algorithm updates the coefficient vector using the FXLMS algorithm expressed as [1]

$$\mathbf{w}(n+1) = \mathbf{w}(n) + \mu\mathbf{x}'(n)e(n), \quad (2)$$

where μ is the step size that determines the stability and convergence of the algorithm, and $\mathbf{x}'(n) = [x'(n)\ x'(n-1)\ \cdots\ x'(n-L+1)]^T$ is the filtered signal vector by the secondary path estimation filter $\hat{S}(z)$. This filtering is expressed as

$$x'(n) = \sum_{m=0}^{M-1} \hat{s}_m x(n-m), \quad (3)$$

where $\hat{s}_m$ is the mth coefficient of $\hat{S}(z)$ of length M. Note that the transfer function $S(z)$ can be estimated by filter $\hat{S}(z)$ using either off-line and/or on-line modeling techniques given in [1].

For perfect cancellation, the error signal should become zero, which requires the adaptive filter to converge to the optimum transfer function expressed as

$$W^o(z) = \frac{P(z)}{S(z)}. \quad (4)$$

Therefore, the adaptive filter models the primary path $P(z)$ and inversely models the secondary path $S(z)$. The behavior and performance of ANC system is mainly determined by the secondary path $S(z)$, which is the target for optimization in this paper. Equation (4) shows that the ANC system is unstable if there is a frequency, ω_0, such that $S(\omega_0) = 0$. In other words, a zero in $S(z)$ at frequency ω_0 means this frequency is uncontrollable since the anti-noise generated by $W(z)$ at that frequency will be attenuated by $S(z)$ before it reaches the summing junction for noise cancellation. These problems will be further discussed in Section 2.3. Therefore, the FXLMS algorithm works properly for all frequencies when the magnitude response of the secondary path is flat. However, the error sensor may not be placed at the optimum location that will have the flat magnitude response of the secondary path. For example, the electronic mufflers used for reducing engine noises have to protect the sensor from high temperature, fast airflow, and a corrosive environment.

This paper develops a new algorithm [10] to solve the problem when the error sensor is not allowed to be placed at the optimum location for obtaining a flat secondary path. In the proposed algorithm, the secondary signal $y(n)$ is pre-filtered by the compensation filter $C(z)$ before being used to drive the secondary source. The filter $C(z)$ reshapes the physical secondary path to approximate the virtual secondary path that places the error microphone at the virtual location. Therefore, we use the signal-processing algorithm to make the ANC system with the error sensor located at the physical location has the desired secondary path such as using the virtual sensor placed at the optimum location.

The approach to move the location of the maximum noise attenuation away from the physical error sensor by using a virtual microphone was developed for ANC in a headset [11] and in a free field [12]. By assuming the spatial rate of the change of the sound pressure between relatively closely spaced locations will be small and predictable, an interpolation or extrapolation was used to estimate the pressures between two measured fixed locations [11, 12]. The prior measurement of the difference of the physical and virtual secondary paths can be used as an operator on the actual error signal to estimate the pressure at the virtual location. This assumption cannot be used for electronic mufflers. In this paper, we develop new modeling techniques for designing the compensation filter $C(z)$ to compensate the physical secondary path such that the overall secondary path approximates the virtual secondary path when the error sensor is placed at the virtual location.

II. ANC SYSTEMS WITH VIRTUAL SECONDARY PATHS

For periodic noise such as those generated by engines, compressors, fans, transformers, and propellers, it is possible to use a nonacoustic sensor to measure the mechanical motion (rpm) for generating an electrical reference signal that contains all the harmonics of the primary noise. This narrowband ANC system avoids the use of a reference microphone close to the engine, and also prevents the acoustic feedback from the secondary source to the reference microphone, thus is the most effective technique for electronic mufflers. In practice, it is also important to protect the error microphone from high temperatures and corrosive environments. The most effective solution is to place the error microphone at the secured location, and use a proper signal-processing algorithm to make the physical error sensor function as the virtual sensor. An important application of a virtual sensor algorithm is the electronic muffler, where the error sensor may not be placed at the desired location.

The concept of using a virtual error sensor can be explained by the narrowband ANC systems with a single error sensor as shown in Figure 3, where the desired

error signal $e'(n)$ is sensed if the error sensor is placed at the virtual location M_v, and $e(n)$ is sensed by the sensor located at the physical location M_p. The location of M_v can be determined by acoustic theory, whereas the location of M_p can be determined by both the acoustic theory and practical considerations for protecting the sensor from hostile environments. For example, the error at the virtual microphone position is lower when the microphone is located in the vicinity of a diffracting surface [11]. The idea of using virtual sensor cannot be directly applied to electronic mufflers since the error sensor is not in a free field. Therefore, the primary source pressure is not the same at both the physical and virtual locations.

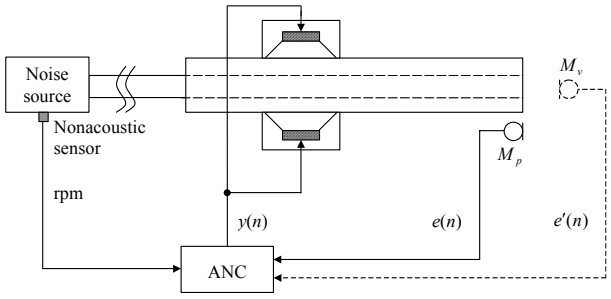

Figure 3 A narrowband ANC system for electronic mufflers with the error sensor at either the virtual location or the physical location

II.1 *Algorithm Derivation*

In this paper, we use $P_p(z)$ and $P_v(z)$ to represent the primary path transfer functions from the noise source to the physical and virtual sensor locations, respectively, and use $S_p(z)$ and $S_v(z)$ to represent the secondary path transfer functions for the physical sensor and virtual sensor, respectively. When the error microphone is placed at the virtual position, the ANC system can be modeled as a block diagram similar to Figure 2, where $P(z)$ is replaced with $P_v(z)$, $S(z)$ is replaced with $S_v(z)$, and $\hat{S}(z)$ is replaced with the estimate $\hat{S}_v(z)$. Similarly, when the microphone is placed at the physical location, $P(z)$ is replaced with $P_p(z)$, $S(z)$ is replaced withy $S_p(z)$, and $\hat{S}(z)$ is replaced with $\hat{S}_p(z)$.

Since the virtual microphone is located at the optimum position, $S_v(z)$ will have a flat magnitude response for the adaptive filter $W(z)$ to achieve optimum performance. The transfer function $S_p(z)$ may not have a flat magnitude response since the error microphone is not placed at the optimum location. As shown in Figure 2, $S_p(z)$ has dips at some frequencies, it will attenuate the anti-noise components at those frequencies before reaching the acoustic summing junction for noise control. As shown in Equation (4), $W(\omega_0)$ has very high gain when $S(\omega_0)$ is small. The filter $W(z)$ may be unstable if an adaptive infinite-impulse response (IIR) filter is used to realize the filter. If an adaptive finite-impulse response (FIR) filter is used, more coefficients are needed to provide high gain at frequency ω_0, thus slows down convergence speed and reduces noise attenuation at other frequencies. A high-order adaptive filter also results in higher complexity, large excess mean-square error, more finite-precision errors, and slower convergence speed. These problems are especially critical for electronic mufflers, because fast convergence is required to track fast changing or engine rpm during accelerations.

The problem of having undesired physical secondary path can be effectively solved by inserting a proper compensation filter $C(z)$ into the secondary path to make the overall secondary path as flat as possible. The new ANC system with virtual secondary path is illustrated in Figure 4, where the filter $C(z)$ is inserted between $W(z)$ and $S_p(z)$ such that the overall secondary path approximates $S_v(z)$. That is,

$$C(z)S_p(z) = S_v(z). \tag{5}$$

The technique of optimizing secondary path has similar effects as placing the error sensor at the virtual location since the primary path has less influence on ANC performance. Therefore, the ANC system with a virtual secondary path uses a signal-processing algorithm to improve noise canceling performance as if the error sensor is placed at the virtual location.

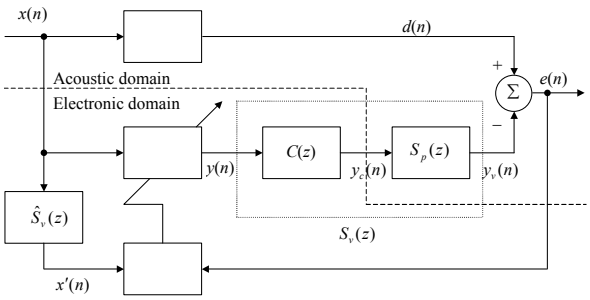

Figure 4 ANC system with virtual secondary path

The algorithm is illustrated in the electronic domain of Figure 4. The input signal $x(n)$ is filtered by $W(z)$ defined in (1). The output signal $y(n)$ is then compensated by $C(z)$ to obtain the secondary noise $y_c(n)$ expressed as

$$y_c(n) = \sum_{j=0}^{J-1} c_j y(n-j), \quad (6)$$

where c_j is the jth coefficient of $C(z)$ of length J. In real-time ANC systems, $y_c(n)$ [instead of $y(n)$] is converted to analog form, amplified, and output to drive the secondary loudspeaker for noise control.

The error signal $e(n)$ sensed by the physical sensor is used to update the coefficients of adaptive filter $W(z)$ using the FXLMS algorithm defined in (2). The signal $x'(n)$ to the LMS block is the filtered output of the transfer function $\hat{S}_v(z)$ expressed as

$$x'(n) = \sum_{m=0}^{M-1} \hat{s}_{v,m} x(n-m), \quad (7)$$

where $\hat{s}_{v,m}$ is the mth coefficient of $\hat{S}_v(z)$ with order M. This single-channel algorithm can be extended to the multiple-channel ANC systems for three-dimensional applications [10].

II.2 Design of Compensation Filter

The compensation filter $C(z)$ equalizes the physical secondary path $S_p(z)$ to allow all the frequency components in the anti-noise to reach the acoustic summing junction for canceling the primary noise. The transfer function of $C(z)$ can be computed from equation (5) as

$$C(z) = \frac{S_v(z)}{S_p(z)} \cong \frac{\hat{S}_v(z)}{\hat{S}_p(z)}, \quad (8)$$

where $\hat{S}_v(z)$ and $\hat{S}_p(z)$ are estimation filters of the secondary paths $S_v(z)$ and $S_p(z)$, respectively. For simulation purposes, the transfer functions $S_v(z)$ and $S_p(z)$ are measured from a prototype electronic muffler that will be explained in the next section. These transfer functions can be modeled by adaptive finite impulse response (FIR) filters $\hat{S}_v(z)$ and $\hat{S}_p(z)$ using off-line modeling techniques [1].

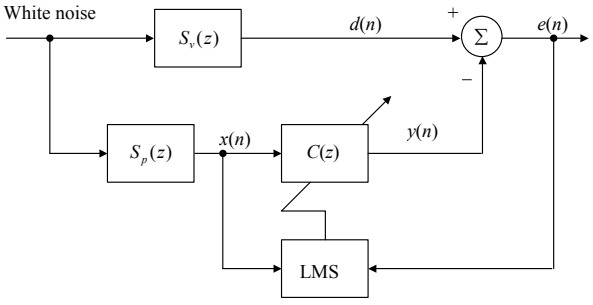

Figure 5 A method to obtain $C(z)$ using FIR filter

An approach to design $C(z)$ using an FIR filter is shown in Figure 5. In this adaptive inverse modeling technique, $S_p(z)$ and $C(z)$ are connected in cascade, and $C(z)$ is an adaptive FIR filter updated by the LMS algorithm. The internal-generated white noise excites $S_v(z)$ to get the desired response $d(n)$. This white noise is also sent through $S_p(z)$ to get $x(n)$, which is then filtered by the adaptive filter $C(z)$ to obtain $y(n)$. After the system converges, we will have $S_p(z)C(z) \approx S_v(z)$, which approximates the desired result defined in (5). The coefficients of $C(z)$ are fixed after convergence and are used for the compensation filter shown in Figure 4 for on-line noise control.

The off-line modeling technique for obtaining $C(z)$ shown in Figure 5 can be realized as the electronic domain algorithm illustrated in Figure 6 for practical ANC applications. The internally generated white noise is amplified to drive the secondary source in the duct. The input signal $x(n)$ for the adaptive filter $C(z)$ is the signal picked up by the physical sensor, while the desired signal $d(n)$ is sensed by the virtual sensor. As shown in Figure 6, the filter output is computed as

$$y(n) = \sum_{j=0}^{J-1} c_j(n) x(n-j) \cdot \quad (9)$$

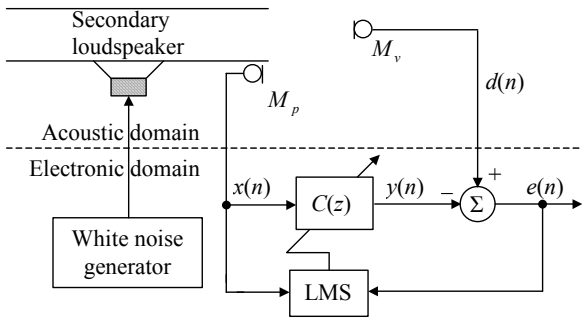

Figure 6 Designing the compensation FIR filter

The error signal is computed as

$$e(n) = d(n) - y(n), \quad (10)$$

and the adaptive filter is adapted by the LMS algorithm expressed as

$$c_j(n+1) = c_j(n) + \mu e(n) x(n-j), \quad j = 0, 1, \ldots, J-1. \quad (11)$$

The magnitude responses of $S_v(z)$, $S_p(z)$, $C(z)$, and $C(z)S_p(z)$ are shown in Figure 7. The virtual secondary path $S_v(z)$ has a satisfactory flat magnitude response. The undesired effects of $S_p(z)$ are compensated by $C(z)$ such that the overall model $C(z)S_p(z)$ approximates $S_v(z)$ as predicted by (8). For example, $S_p(z)$ has a dip at approximately 370 Hz that will attenuate the anti-noise, thus the ANC system is ineffective in canceling the primary noise at that frequency using the physical error microphone. As shown in Figure 7(c), the

compensation filter $C(z)$ has a peak at 370 Hz to equalize the undesired dip. Therefore, the performance of ANC system with a virtual secondary path is equivalent to the error microphone being placed at the virtual location.

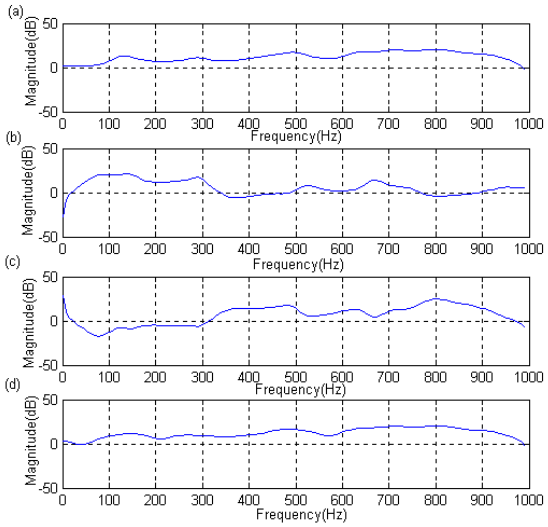

Figure 7 Magnitude responses of (a) $S_v(z)$, (b) $S_p(z)$, (c) $C(z)$, and (d) $C(z)S_p(z)$

II.3 Analysis of Virtual Secondary Path

By taking the z-transform of signals in the electronic domain of Figure 4, we can derive the optimum solution of the adaptive filter as

$$W^o(z) = \frac{P_p(z)}{C(z)S_p(z)}. \quad (12)$$

From (5), $C(z)S_p(z) = S_v(z)$, we thus have

$$W^o(z) = \frac{P_p(z)}{S_v(z)}. \quad (13)$$

Note that the steady-state solution is related to $P_p(z)$ instead of $P_v(z)$. Therefore, the ANC system still minimizes the pressure at the physical error sensor location instead of the virtual sensor location. The optimum performance at the virtual sensor location cannot be guaranteed. However, the performance of ANC system is mainly determined by the secondary path. With the virtual secondary path $S_v(z)$ in Equation (13), the performance of this adaptive system is similar to the ANC system that uses a virtual sensor at the optimum location.

In order to verify Equation (12), white noise is used as input $x(n)$ to the ANC system shown in Figure 4. After the convergence of the adaptive filter $W(z)$, the magnitude response of $W^o(z)C(z)S_p(z)$ is shown in the top plot of Figure 8. The magnitude response of $P_p(z)$ is shown in the bottom plot of Figure 8, which is similar to the top plot. Therefore, Equation (12) is verified by computer simulations.

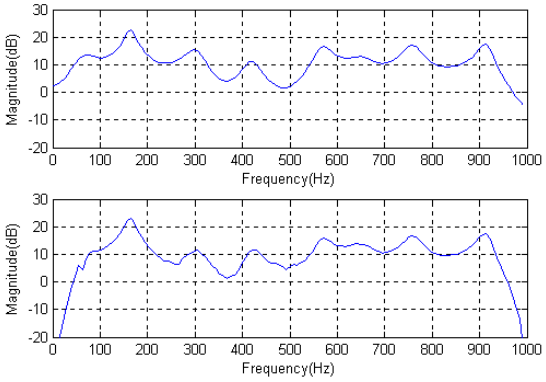

Figure 8 Magnitude responses of $P_p(z)$ (top plot) and $W^o(z)C(z)S_p(z)$ (bottom plot)

The new ANC system with virtual secondary path shown in Figure 4 increases computations by using an extra compensation filter $C(z)$. This requires additional J multiplications and J–1 additions, where J is the length of the filter $C(z)$. In addition, a more complicated program is needed to estimate $C(z)$ as shown in Figure 6. However, this is done during the off-line modeling, thus will not increase computational requirements for on-line ANC in real time. As discussed in Section 2.1, using a fixed filter $C(z)$ requires less computation than using a high-order adaptive filter $W(z)$, since updating the filter coefficients using the FXLMS algorithm need more computation.

III. EXPERIMENT AND SIMULATION RESULTS

A practical ANC system in an electronic muffler has been built and used to estimate the primary- and secondary-path transfer functions. Computer simulations based on these transfer functions are performed to evaluate the performance of the new ANC system shown in Figure 4 at the physical sensor in comparison with the traditional ANC system without using the virtual secondary path.

III.1 Electronic Mufflers

A prototype electronic muffler made up of stainless steel pipes is built for testing the ANC systems. Figure 9(a) shows the side view of the muffler, and the top view is depicted in Figure 9(b). As shown in Figure 9, there are two ducts in the muffler. The outer duct has a diameter of 21 cm and a length of 76 cm. There is a small narrow duct inside the outer duct, which has a length of 89 cm and a diameter of 5 cm. A small portion of the inner duct with a length of 13 cm is outside the main muffler, which will be connected to the exhaust system from an engine. Two secondary loudspeakers are placed inside the side ducts, which are connected perpendicularly to the muffler's outer duct. The ANC system uses two loudspeakers that are connected

together to prevent overdriving the loudspeakers. Primary noise from the left side travels to the right along the inner duct, while the secondary noise travels along the outer duct. The primary noise in the middle is superimposed with the surrounding primary noise at the end of the muffler as shown in Figure 9(b). In this configuration, the secondary loudspeakers are protected from the high temperature exhaust inside the inner duct.

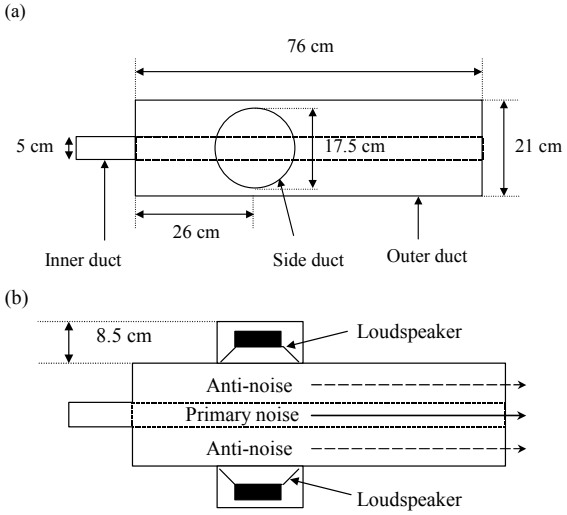

Figure 9 The prototype electronic muffler used for experiments. (a) Side view, and (b) top view

The equipment used for the experiments includes an HP3563A control systems analyzer, which generates the random noise for system identification, and estimates the poles and zeros of the primary- and secondary-path transfer functions. Two 6" Kicker loudspeakers are used as secondary sources, which are connected together to produce anti-noise that is amplified by a dual-channel QSC MX-700 power amplifier. A Shure Brothers SM98 microphone is used as the error sensor, and a dual-channel Symetrix SX202 preamplifier is used for the microphone signal.

III.2 Estimation of Transfer Functions

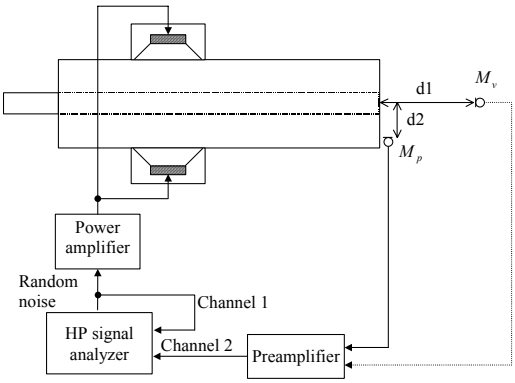

Figure 10 Setup for measuring $S_v(z)$ and $S_p(z)$

In order to simulate the virtual sensor algorithm for the electronic muffler, we need the primary-path transfer function $P_p(z)$ and the secondary-path transfer functions $S_v(z)$ and $S_p(z)$. As illustrated in Figure 10, the random noise generated by HP signal analyzer is used as an excitation signal for modeling the required physical plants. The generated random noise is connected to the Channel 1 input of the signal analyzer, and the same noise is amplified by the power amplifier for driving the secondary loudspeakers. The error microphone M_v output is connected to the HP analyzer's Channel 2 input for estimating the transfer function $S_v(z)$. The sampling frequency is set to 2 kHz.

The HP analyzer estimates the poles and zeros of the primary and secondary paths. The poles and zeros obtained from the analyzer are converted to polynomial form by a MATLAB program for computer simulations. To obtain a flat magnitude response of $S_v(z)$, the position of the error microphone may be determined by acoustic theory [3, 4, 11, 12]. In this research, we change the error microphone location for estimating different transfer functions corresponding to those locations. As shown in Figure 10, the distance d1 from the end of inner duct to M_v is varied for measuring different magnitude responses of $S_v(z)$ as shown in Figure 11. The magnitude response of $S_v(z)$ is most flat when the distance d1 is 28 cm from the end of the pipe to the error microphone. This position is assumed to be an optimum virtual sensor location, and the corresponding transfer function will be used for computer simulations of ANC systems with virtual sensors. Note that it is very difficult to place the error sensor at this optimum location for practical electronic mufflers.

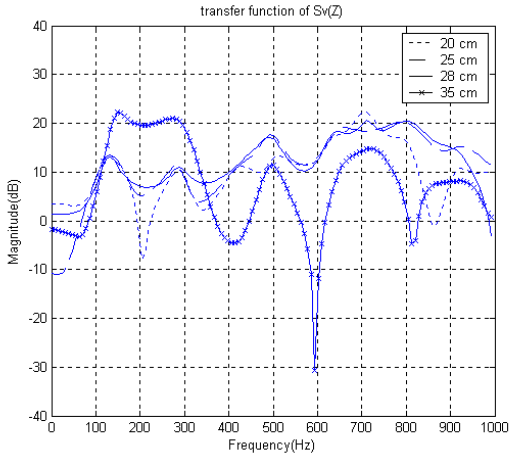

Figure 11 Magnitude responses of $S_v(z)$ at different virtual error sensor locations

The experimental setup shown in Figure 10 can be used for measuring $S_p(z)$ by moving the error microphone from the virtual location M_v to the physical location M_p. The distance d2 is varied to get different transfer functions of $S_p(z)$. The magnitude responses of $S_p(z)$ for the physical error microphone M_p at various positions are shown in Figure 12, which shows that the distance d2 = 8.9 cm has relatively flat magnitude response. It is important to note that this distance allows the error sensor to be placed inside the outer duct for protection in real-world applications. Thus this estimated transfer function would be used for computer simulations.

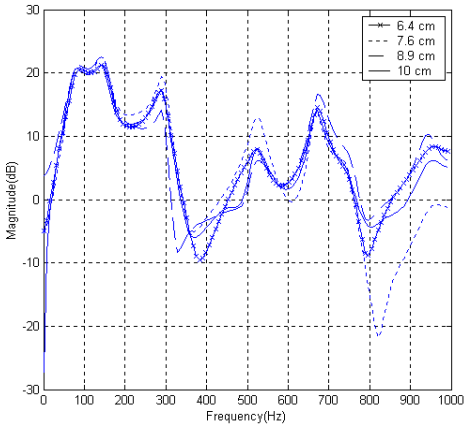

Figure 12 Magnitude responses of $S_p(z)$ at different physical microphone positions

In order to estimate the primary-path transfer function $P_p(z)$, the electronic muffler shown in Figure 10 is connected to a noise source, which is a loudspeaker inside the speaker box with a PVC pipe as the noise outlet. The PVC pipe and the muffler are sealed tightly to avoid signal leak at the connection. Random noise generated by the HP analyzer is sent to the primary noise source instead of the secondary loudspeakers as shown in Figure 10. This random noise is also connected to the Channel 1 input of the analyzer. The process of getting $P_p(z)$ is the same as estimating the secondary path transfer functions introduced earlier.

III.3 Computer Simulations

In order to simulate the ANC system with a virtual secondary path as shown in Figure 4, we need the transfer functions $P(z)$, $C(z)$, $S_p(z)$, and $\hat{S}_v(z)$. The transfer functions $P_p(z)$ and $S_p(z)$ are obtained by experiments given in Section 3.2, and the transfer function $\hat{S}_v(z)$ is obtained by off-line modeling of $S_v(z)$ using an adaptive FIR filter with the LMS algorithm [1]. The transfer function $C(z)$ is obtained by the off-line modeling technique given in Figure 5 with smaller step sizes for a larger number of samples. As shown in Figure 11, the virtual secondary path $S_v(z)$ has a desired flat magnitude response when compared to the physical secondary path $S_p(z)$ shown in Figure 12. The compensation filter $C(z)$ inverts the dips of $S_p(z)$ such that the overall model $C(z)S_p(z)$ approximates to $S_v(z)$ as shown in Figure 7.

The traditional ANC system without using the virtual secondary path can be simulated by replacing the transfer function $S_v(z)$ with $S_p(z)$ in Figure 4. If the primary signal has frequency components at the dips of the magnitude response of $S_p(z)$ as shown in Figure 12, the physical secondary path will attenuate these frequency components. Therefore, the frequency components in the primary noise cannot be canceled properly by the traditional ANC systems. Note that the virtual sensor algorithm with $P_v(z)$ and $S_v(z)$ can be simulated by replacing $P_p(z)$ with $P_v(z)$ in Figure 4.

For the new ANC algorithm with virtual secondary path as shown in Figure 4, the transfer function $C(z)$ will compensate $S_p(z)$ to make the overall transfer function $C(z)S_p(z)$ approximates to $S_v(z)$. As shown in Figure 7(d), the overall secondary path has flat magnitude response, thus the ANC system is able to cancel the primary noise components at those frequencies. This improvement can be verified by using the input sinusoidal signal with frequency components at the dips of $S_p(z)$.

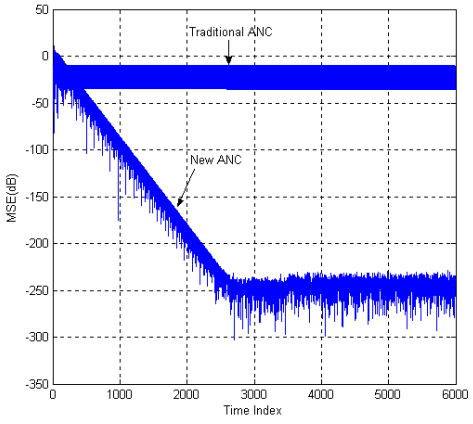

Figure 13 Squared errors of ANC systems when the sinewave frequency is at the dip of $S_p(z)$

As shown in Figure 12, there is a significant dip at 375 Hz, thus a sinewave signal at that frequency is used as input $x(n)$ to evaluate the performance of the

optimized ANC system with virtual secondary path in comparison with the traditional ANC system at the physical error sensor location. Different filter orders and step sizes are tested for achieving best performance. For the traditional ANC system, the length of the adaptive filter is $L = 256$, and the step size is $\mu = 0.000004$. For the new ANC system, the length of the filter is $L = 128$, and the step size is $\mu = 0.00016$. This result verifies that the new algorithm needs lower-order adaptive FIR filter with larger step size for faster convergence. The squared residual noises for both ANC systems are shown in Figure 13. It shows that the performance of the ANC system with a virtual secondary path is much better than that of the traditional ANC system when the primary noise has frequency components at the dips of $S_p(z)$. This is because the transformation filter $C(z)$ compensates the adverse effects as shown in Figure 7.

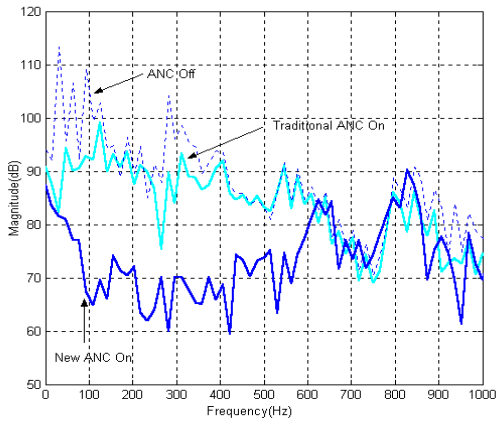

Figure 14 Performance of ANC systems with a real engine noise

The new ANC system and the traditional ANC system for the practical electronic mufflers were further tested using real engine noise. The engine noise is recorded from a welding generator running at low idle speed of 2,200 rpm [13], and the sampling frequency is 2 kHz. The spectrum of the original engine noise when the ANC system is turned off is compared with the spectra of the residual error signals from the traditional ANC and the new ANC. As shown in Figure 14, both ANC systems are able to attenuate the undesired engine noise, however, the new ANC system achieves additional 20 dB at frequency range 100 to 400 Hz as shown in Figure 14. The traditional ANC was able to attenuate narrowband components of the engine noise by 20 dB, while the new ANC system able to further reduce broadband noise at frequencies below 600 Hz. The new ANC system was able to attenuate the engine noise by a significant amount when compared to the traditional ANC system.

IV. CONCLUSIONS

This paper developed a new algorithm for ANC systems with virtual secondary paths to optimize the performance of systems when the sensors must be placed at a non-optimal, secured location to protect the sensor from high temperature, fast airflow, and a corrosive environment for real-world applications. The new ANC algorithm introduced a compensation filter and its design techniques such that the overall secondary path equivalent to the placement of error sensor at the optimum virtual location. A practical ANC system in the electronic muffler was built and used to verify the performance improvement by using this new technique. The algorithm can also be used in other ANC systems where the secondary path transfer function is not flat because of practical constraints on sensor placement.

V. REFERENCES

[1] S. M. Kuo and D. R. Morgan, *Active noise control systems*: *Algorithms and DSP implementations*, New York, NY: John Wiley & Sons, 1996.

[2] S. M. Kuo and D. R. Morgan, "Active noise control: A tutorial review," *Proc. of the IEEE*, vol. 87, pp. 943-973, June 1999.

[3] P. A. Nelson and S. J. Elliott, *Active control of sound*, San Diego, CA: Academic Press, 1992.

[4] C. H. Hansen and S. D. Snyder, *Active control of noise and vibration*, London, U.K.: E&FN Spon, 1997.

[5] S. M. Kuo and W. S. Gan, *Digital signal processors*, Upper Saddle River, NJ: Prentice Hall, 2004.

[6] B. Widrow and S. D. Stearns, *Adaptive signal processing*, Englewood Cliffs, NJ: Prentice-Hall, 1985.

[7] D. R. Morgan, "An analysis of multiple correlation cancellation loops with a filter in the auxiliary path," *IEEE Trans. Acoust., Speech, Signal Processing*, vol. ASSP-28, pp. 454-467, Aug. 1980.

[8] B. Widrow, D. Shur, and S. Shaffer, "On adaptive inverse control," *in Proc. 15th Asilomar Conf.*, 1981,pp.185-189.

[9] J.C. Burgess, "Active adaptive sound control in a duct: A computer simulation," *J.Acoust. Soc. Am.*, 70, 715-726, September 1981.

[10] S. Kalluri, *Virtual sensors in active noise control systems*, MS thesis, Northern Illinois University, Dec. 2003.

[11] J. Garcia-Bonito, S. J. Elliott, and C. C. Boucher, "Generation of zones of quiet using a virtual microphone arrangement," *J. Acoust. Soc. Am.*, vol. 101, no. 6, pp.3498-3516, June 1997.

[12] C. D. Kestell, B. S. Cazzolato, and C. H. Hansen, "Active noise control in a free field with virtual sensors," *J. Acoust. Soc. Am.*, vol. 109, no. 1, pp. 232-243, January 2001.

[13] S. M. Kuo, X. Kong, and W. S. Gan, "Applications of adaptive feedback active noise control system," *IEEE Trans. Control Systems Technology*, vol. 11, no. 2, pp. 216-220, March 2003.